Optical Alignment of the High-Precision UV Spectro-Polarimeter (CLASP2)

Donguk Song[a,*], Ryohko Ishikawa[a], Ryouhei Kano[a], Masaki Yoshida[b], Toshihiro Tsuzuki[a], Fumihiro Uraguchi[a], Kazuya Shinoda[a], Hirohisa Hara[a], Takenori J. Okamoto[a], Frédéric Auchére[d], David E. McKenzie[c], Laurel A. Rachmeler[c], and Javier Trujillo Bueno[e]

[a]National Astronomical Observatory of Japan, 2-21-1 Osawa, Mitaka, Tokyo 181-8588, Japan
[b]Department of Astronomical Science, Graduate University for Advanced Studies (SOKENDAI), Tokyo 181-8585, Japan
[c]NASA Marshall Space Flight Center, Huntsville, AL 35812, USA
[d]Institut d'Astrophysique Spatiale, CNRS/Univ. Paris-Sud 11, Batiment 121, 91405 Orsay, France
[e]Instituto de Astrofísica de Canarias, E-38205 La Laguna, Tenerife, Spain

ABSTRACT

Chromospheric LAyer Spectro-Polarimeter (CLASP2) is our next sounding rocket experiment after the success of Chromospheric Lyman-Alpha Spectro-Polarimeter (CLASP1). CLASP2 is scheduled to launch in 2019, and aims to achieve high precision measurements of the linear and circular polarizations in the Mg II h & k lines near the 280 nm, whose line cores originate in the upper solar chromosphere. The CLASP2 spectro-polarimeter follows very successful design concept of the CLASP1 instrument with the minimal modification. A new grating was fabricated with the same radius of curvature as the CLASP1 grating, but with a different ruling density. This allows us to essentially reuse the CLASP1 mechanical structures and layout of the optics. However, because the observing wavelength of CLASP2 is twice longer than that of CLASP1, a magnifier optical system was newly added in front of the cameras to double the focal length of CLASP2 in order to maintain the same wavelength resolution as CLASP1 (0.01 nm). Meanwhile, a careful optical alignment of the specto-polarimeter is required to reach the 0.01 nm wavelength resolution. Therefore, we established an efficient alignment procedure for the CLASP2 spectro-polarimeter based on an experience of CLASP1. Here, we explain in detail the methods for achieving the optical alignment of the CLASP2 spectro-polarimeter and discuss our results by comparing with the performance requirements.

Keywords: Chromospheric magnetic field, UV spectropolarimeter, Optical alignment

1. INTRODUCTION

The advanced UV spectropolarimeter called the Chromospheric Lyman-Alpha Spectro-Polarimeter[1] (hereafter, CLASP1) was launched by a NASA sounding rocket in 2015. It explored the magnetic fields in the upper chromosphere and the transition region. In particular, it successfully measured the linear polarization for the first time which is produced by the scattering processes and the Hanle effect in the hydrogen Lyman-alpha line at 121.57 nm[2] and in the Si III line at 120.65 nm.[3] The payload of the CLASP1 instrument was fully recovered after its flight and will be relaunched in 2019 under the new name of the Chromospheric LAyer Spectro-Polarimeter[4] (hereafter, CLASP2).

The scientific goal of CLASP2 is also to advance our empirical knowledge of the magnetic fields in the upper solar chromosphere. However, in CLASP2, we will observe the Sun by using the Mg II h & k lines near the 280 nm. The intensity of the Mg II h & k line cores mainly originates in the upper chromosphere. Since 2013, the high-resolution observations in the Mg II h & k lines enabled by the Interface Region Imaging Spectrometer[5]

Further author information: (Send correspondence to Donguk Song)
Donguk Song: E-mail: donguk.song@nao.ac.jp, Telephone: +81-422-34-3724

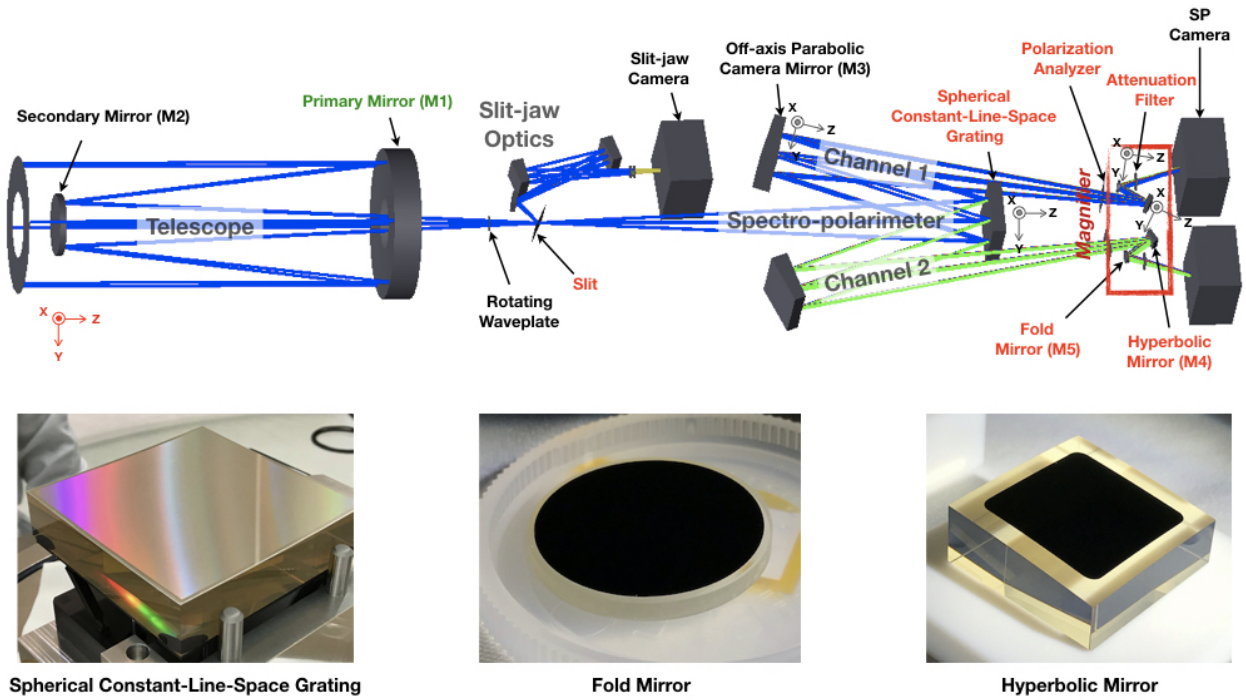

Figure 1. Top: Optical design of the CLASP2 instrument. The coordinate system marked as red and gray arrows respectively represents the coordinate system of the CLASP1 mechanical axis and each optical component in the spectro-polarimeter. Black letters present reused optical elements from the CLASP1 instrument, while red letters show the new optics for the CLASP2. In addtion, the green letter indicates the re-coated mirror. Bottom: new optical components for the CLASP2 spectro-polarimeter.

(IRIS) have advanced our knowledge of dynamics and heating phenomena in the solar atmosphere. However, their polarization properties are relatively unknown. The theoretical studies on the polarization in the Mg II h & k lines predicted that the linear polarization in the core of the Mg II k line is caused by the Hanle effect.[6–8] Circular polarization by the Zeeman effect can be induced in both Mg II h & k lines. Moreover, magneto-optical effects introduce an interesting magnetic sensitivity in the wings of Mg II h & k lines. By using these spectral lines, CLASP2 will be able to achieve high precision measurements of the circular and linear polarizations by the joint action of scattering processes and the Hanle and Zemman effects

To this end, we refurbished the existing CLASP1 spectro-polarimeter in order to optimize the image quality at the Mg II h & k lines, and fabricated new optical elements and their mounting structures. In addition, we established and performed an efficient optical alignment of the spectro-polarimeter. In this paper, we explain the new design of the spectro-polarimeter of CLASP2. We also describe the methods for achieving the optical alignment of the CLASP2 spectro-polarimeter in detail and discuss our results by comparing with the performance requirements.

2. DESIGN OF THE SPECTROPOLARIMETER

The CLASP2 spectro-polarimeter (SP) follows the very successful design concept of the CLASP1 instrument.[1] It is composed of two channels that are optically symmetric (Figure 1). This allows to measure the orthogonal states of polarizations using both ±1st order beams diffracted by a spherical constant-line-space grating, simultaneously.

Because the CLASP1 instrument was fully recovered after the flight, we refurbished the CLASP2 spectro-polarimeter with minimal modification from such an instrument in order to measure the four Stokes parameters by using the Mg II h & k lines near the 280 nm. First, the spherical grating was replaced by new one with the same radius of curvature and diameter as the CLASP1's grating, but with a different ruling density 1303 lines mm^{-1}.

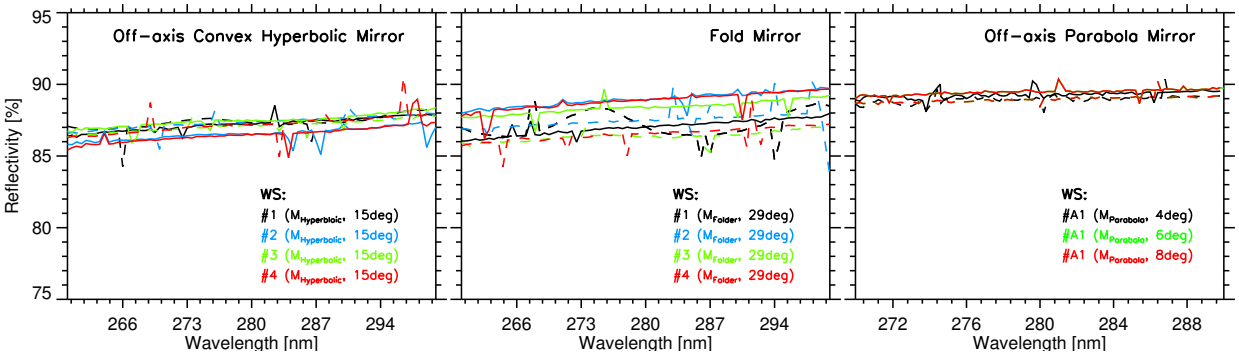

Figure 2. Measured reflectivity of the witness samples (WSs) of the off-axis convex hyperbolic mirror (left), the fold mirror (middle), and the off-axis parabolic mirror (right). The dashed and solid lines represent p- and s-polarized light, respectively.

This enabled that the dispersed beam from the grating has the same exit angle as CLASP1. It allows us to reuse most of the CLASP1 mechanical structures and the optical components such as an off-axis parabolic mirror. Second, we use the transmissive polarization analyzer that is the wire grid linear polarizer in order to achieve higher efficiency in the near ultraviolet.[9] We installed the polarization analyzer on each channel so that the principal axes are parallel or perpendicular to the ruling direction of the grating. This allows us to measure two orthogonal polarizations at the same time. Third, a magnifier optical system was newly designed and installed after the polarization analyzer (red box in Figure 1). It is composed of the off-axis convex hyperbolic mirrors (M4) and the fold mirrors (M5). Because the observing wavelength of CLASP2 is twice longer than that of CLASP1, the magnifier optical system in front of the cameras effectively doubles the focal length of CLASP2 to keep the wavelength resolution as high as the CLASP1 instrument (0.01 nm). In addition, we designed a new camera bracket (hereafter, CLASP2 camera bracket) to maintain the magnifier optical system as a single unit in the CLASP2 SP structure.

Table 1. Specifications of the CLASP2 spectropolarimeter[4]

Spectrograph Type	Inverse Wadsworth Mounting
Grating Type	Spherical constant-line-space with the grove density of 1303 line mm^{-1}
Spectral window	Otimized for the Mg II h (280.35 nm) & k (279.64 nm) lines
Detector	512 × 512 CCD, 13 μm pixel
Plate scale	0.529arcsec/pixel (Spatial) & 0.005 nm/pixel (Spectral)
Slit	7 μm (width) × 2.5 mm (length)

The new mirrors of M4 and M5 were fabricated by CLEARCERAM that is a glass-ceramic with an ultra-low thermal expansion coefficient, and then applied to the Al+MgF_2 coating to improve the reflectivity (R) over the wavelength range of 280 ± 1 nm at the required angle of incidence (AOI): the convex hyperbolic mirror (R > 80 % at the 11° - 18° of the AOI) and fold mirror (R > 80 % at the 24° - 33° of the AOI). We confirmed the coating reflectivity not only for the new mirrors (M4 & M5) but also for the old mirror of the spectro-polarimeter (i.e., M3) around 280 nm by using their witness samples at the Ultraviolet Synchrotron Orbital Radiation Facility (UVSOR) of the Institute for Molecular Sciences. The witness samples are 1-inch flat mirrors coated at the same time as the flight mirrors during the coating processes. The measured reflectivity of all witness samples is larger than 85 % at the predetermined AOIs (Figure 2). Our results indicate that new mirrors fabricated for CLASP2 satisfy our requirement. The right panel of Figure 2 also shows that the off-axis parabolic mirror that had been coated with Al+MgF_2 during the CLASP1 experiment keeps enough reflectivity (∼ 89 %) near the 280

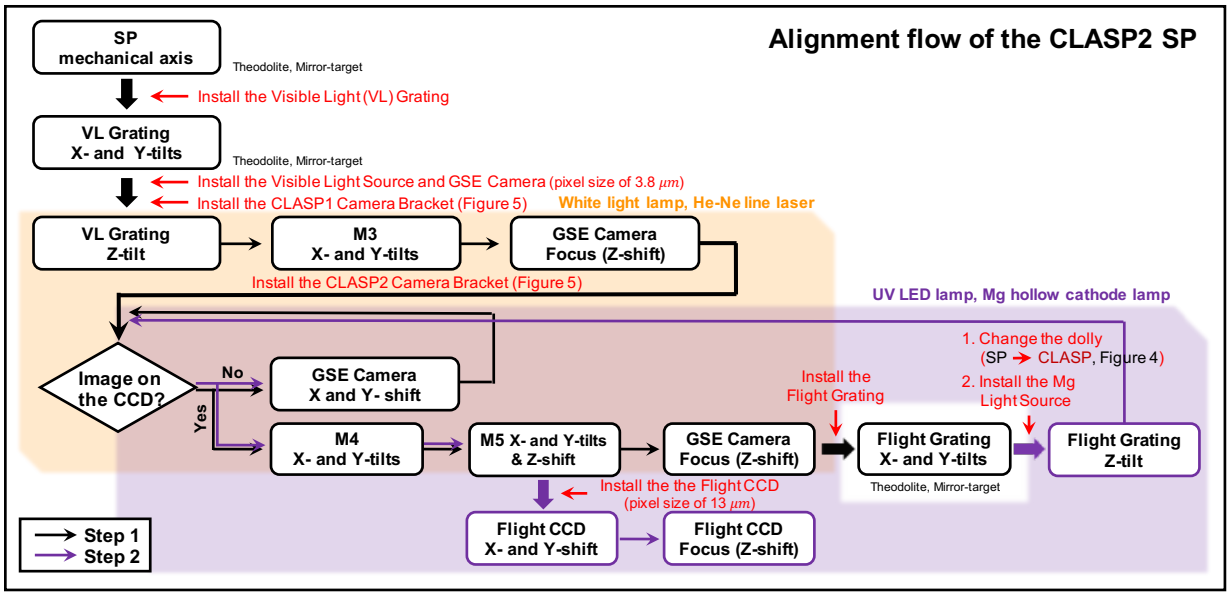

Figure 3. Optical alignment flow of the CLASP2 spectro-polarimeter. Black arrows (step1) present the alignment by using the He-Ne laser (632.8 nm), and violet arrows (step2) indicate the alignment by using the Mg hollow cathode lamp. The installation of optics and the experiment configuration represent with the red arrows.

nm wavelength. Note that, this witness sample is accompanied with the CLASP1/CLASP2 instrument except the CLASP1's launch in order to monitor its degradation of the coating. After the flight of CLASP1, we have performed the reflectivity measurement of the M3's witness sample two times near the 280 nm wavelengths: at the first experiment in 2015, we had confirmed that its reflectivity was about 88 %, and at the second experiment in 2017, we also confirmed that the measured reflectivity is about 89 %. It indicates that there is no significant degradation of coating performance after the flight of CLASP1.

In addition, we fabricated a new slit-mirror whose gap is 7 μm × 2.5 mm, because the slit-mirror of CLASP1 (18.4 μm × 5.1 mm) is too wide to satisfy our required spectral resolution of CLASP2. We also performed the Al+MgF_2 coating on the mirror surface to have the high reflectivity at 122 nm for the slit-jaw system. The slit-jaw system will remain unchanged from the first flight to take Lyman-alpha images in the upper solar chromosphere with the fast-cadence of 0.6 s.[10,11] It will also use to confirm targeting during flight.

3. OPTICAL ALIGNMENT OF THE SPECTRO-POLARIMETER

The CLASP2 spectro-polarimeter aims the measurement of the circular and linear polarization in the Mg II h (280.35 nm) & k (279.64 nm) lines at the high precision (< 0.1 %) and the high spectral resolution (< 0.01 nm). For this, a careful alignment of the SP optics for each channel is required. Table 2 shows the difference between CLASP1 and CLASP2 for the alignment of the spectro-polarimeter. Unlike the spectral window of CLASP1 around 121.6 nm, the Mg II h & k spectral lines are not absorbed in air, so the optical alignment of the CLASP2 spectro-polarimeter can be performed in air, which made the experiment more easier. However, the addition of the magnifier optical system has resulted in an increase of degrees of freedom in the alignment of the CLASP2 spectro-polarimeter. Based on the tolerance analysis, we have chosen for each channel eleven degrees of freedom. Seven degrees of freedom (grating's X-, Y-, and Z-tilts; X- and Y-tilts of the off-axis parabolic mirror (M3); X- and Y-tilts of the off-axis convex hyperbolic mirror (M4)) are related to the adjustment of the image quality, and two degrees of freedom (X- and Y-tilts of the fold mirror (M5)) are connected to the image shift on the CCD camera, while the other two degrees of freedom (CCD defocus along the Z-axis; Z-shift of the fold mirror (M5)) are associated with the adjustment of the focus position of the CCD camera. Such degrees of freedom of each mirror are complicatedly linked together. Furthermore, the Mg hollow cathode lamp and the UV LED lamp that we employ as Mg II h & k light source are so faint. To solve such issues, we established an efficient

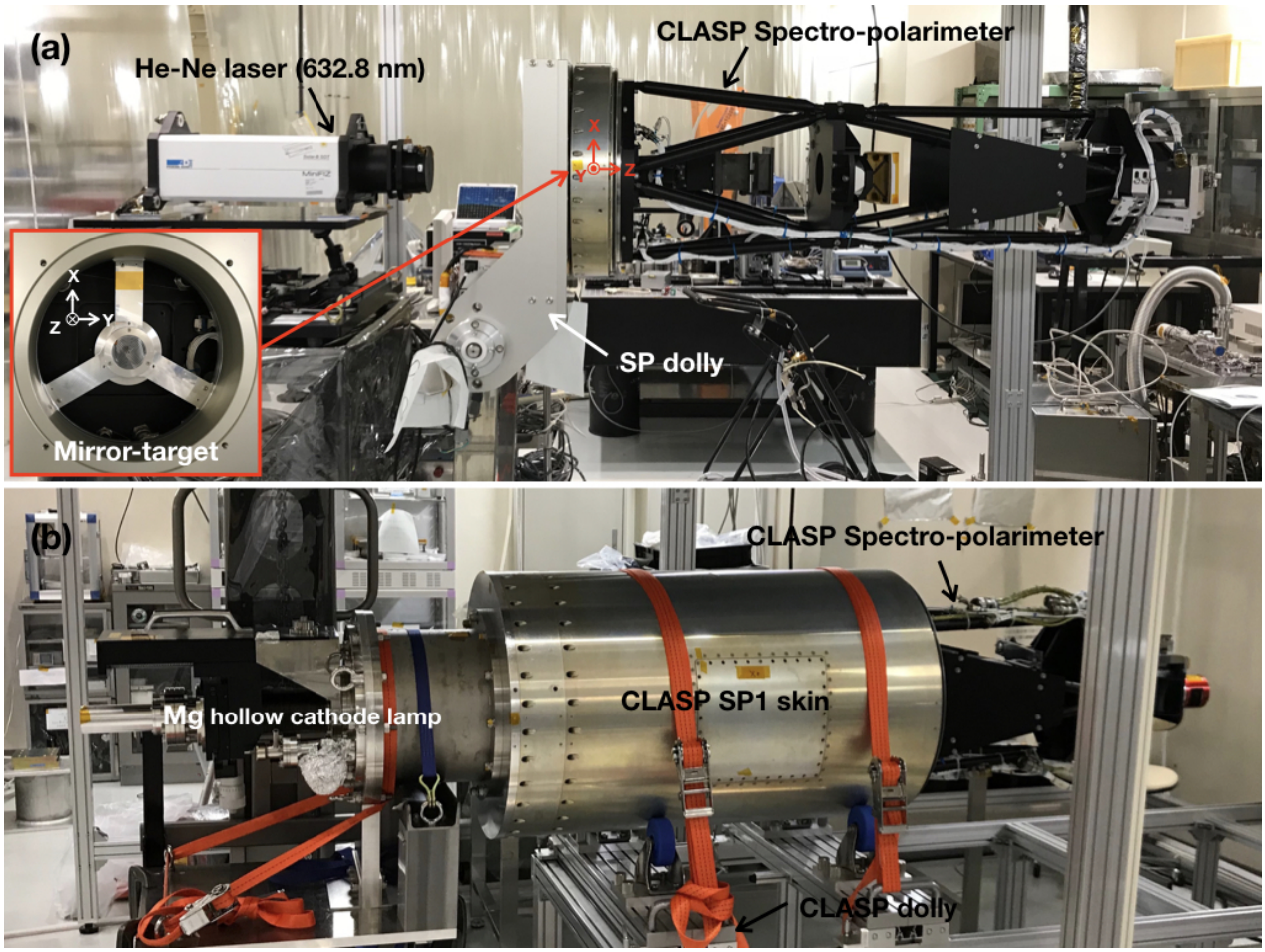

Figure 4. Two experiment configurations for the alignment of the spectro-polarimeter: (a) SP dolly for the SP alignment with the VL light source (He-Ne laser and white-light LED lamp) and (b) CLASP dolly for the SP alignment with the Mg light source (Mg hollow cathode lamp and UV LED lamp). To define the SP mechanical axis, we used the mirror-target (red box) that is installed at the entrance of the SP.

alignment procedure (Figure 3) of the CLASP2 spectro-polarimeter based on the experience[12] of the CLASP1 spectro-polarimeter: (1) we define the SP mechanical axis (red coordinate system in Figure 1) and adjust the X- and Y-tilts of gratings by using the theodolite. (2) To minimalize the alignment with the flight grating and the Mg II light source, we performed the alignment as two steps (Figure 3). First, we carried out the alignment as much as possible with the He-Ne laser (632.8 nm) by using the custom-made grating (hereafter, VL grating), and then performed the fine alignment by using the Mg II light source and the flight grating. (3) To distinguish the effects of the image quality due to the misalignment of M3 and M4, we used two different camera brackets (Figure 5). One is the CLASP1 camera bracket that only includes a reflective polarization analyzer with the plane surface, the other is the CLASP2 camera bracket that consists of M4 and M5.

3.1 Definition of the SP Mechanical Axis

In order to align the CLASP2 spectro-polarimeter (SP), we disintegrated the telescope and installed the spectro-polarimeter on a dolly ("SP dolly" in upper panel of Figure 4). Then, we defined the SP mechanical axis based on a mirror-target that consists of concentric rings of the coated and uncoated areas. The mirror-target was installed at the entrance of the spectro-polarimeter. Here, the center of the mirror-target represents the origin of the SP mechanical X- and Y-axes and the normal of the mirror-target represents the SP mechanical Z-axis

Table 2. Difference between the CLASP1 and CLASP2 for the alignment of the spectro-polarimeter. M3, M4, and M5 are SP mirrors of an off-axis parabola mirror, an off-axis convex hyperbolic mirror, and a folder mirror, respectively.

	CLASP1	CLASP2
Light source	Lyman-alpha (121.6 nm)	Mg II h (280.35 nm) & k (279.64 nm)
Optical elements	Grating, M3, CCD	Grating, M3, M4, M5, CCD
Degrees of freedom	Grating (X-, Y- and Z-tilts) M3 (X- and Y-tilts) CCD defocus (Z-shift)	Grating (X-, Y-, and Z-tilts) M3 (X- and Y-tilts) M4 (X- and Y-tilts) M5 (X- and Y-tilts & Z-shift) CCD defocus (Z-shift)
Pinhole array	ϕ 10 μm $\times$ 5 ($\pm$200″, $\pm$100″, 0″)	ϕ 7 μm $\times$ 5 ($\pm$100″, $\pm$50″, 0″)
Experiment environment	air & vacuum	air

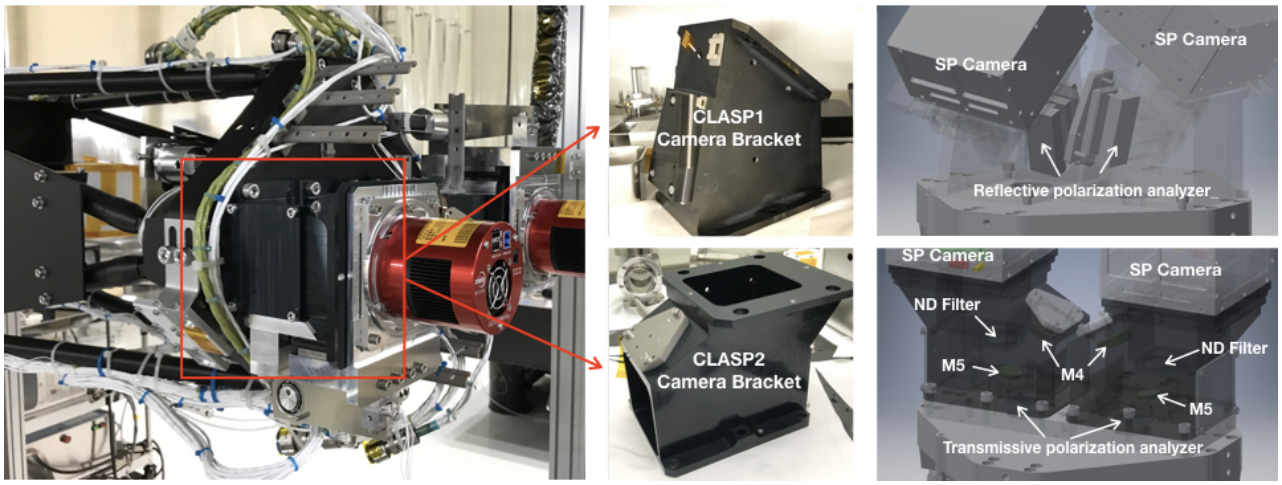

Figure 5. Two camera brackets of the CLASP1 (Top) and the CLASP2 (Bottom). Right panels show the installed optical components inside each camera bracket.

(Red coordinate system of Figure 1). We set-up a theodolite in front of SP dolly and adjusted its X- and Y-titls and positions based on the SP mechanical axis. As a result, the theodolite represents the SP mechanical axis.

3.2 Alignment with the Visible Light Grating

We installed a VL grating for the first step of the SP alignment (Figure 3). The VL grating has the same clear aperture and the curvature radius with the flight grating. The dispersed beam into the $\pm$1st order at the VL grating has the same diffraction angle in the He-Ne line (632.8 nm) as the diffraction angle of the flight grating at 279.9 nm that is the mean wavelength of the Mg II h & k lines. Based on the theodolite installed in front of the SP dolly, the VL grating's X- and Y-tilts were aligned to the SP mechanical axis by shimming under the grating holder. Their residuals are 0.21′ in X and 0.17′ in Y, which are smaller than our tolerance ranging of 0.3′.

Meanwhile, the Z-tilt of the VL grating was adjusted so that the relative angle between the slit direction and the dispersion direction are perpendicular to each other in both channels. Note that, the dispersion direction changes depending on the Z-tilt of the grating since it leads to the change of ruling direction. For this, we used two different VL light sources of the He-Ne laser (632.8 nm) to know the slit direction and the white-light LED lamp to show the dispersion direction. In addition, we used a pinhole array that has five pinholes ($\phi \sim 7$ μm)

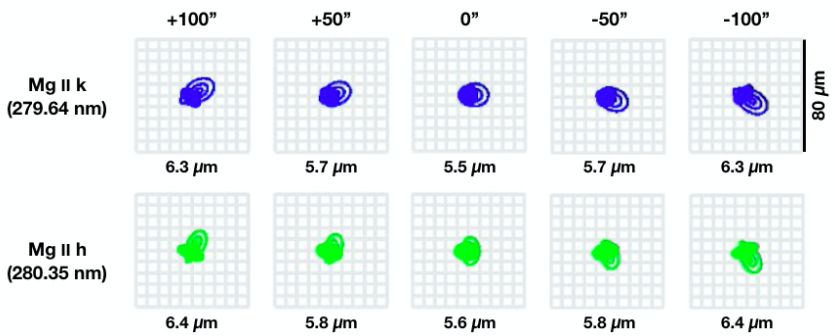

Figure 6. Spot diagrams of the Mg II h (green) & k (blue) lines taken by the channel1 of the CLASP2. The horizontal pannels show the field of view of the pinhole array. The RMS spot diagrams of channel2 have the same shapes with those of channel1, but show the different orientation because of the symmetry of the spectro-polarimeter.

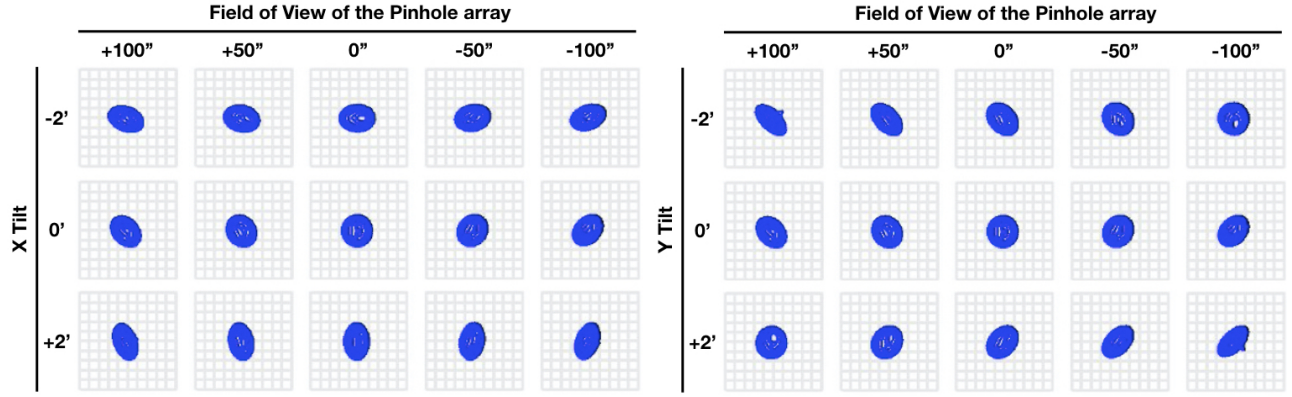

Figure 7. Spot diagrams of the channel 1 in the Mg II k line (279.64 nm) at the -400 μm focus position of the CCD camera when M3 has the misalignment of the X- (left) and Y- (right) tilts: -2, 0, and +2. The misalignment of the M4s X- and Y-tilts also show the same behaviours.

with an interval of 0.625 mm along the slit direction, corresponding to the FOV of +100”, +50”, 0”, -50”, -100” instead of the slit. The angle between the slit and dispersion directions was finally adjusted to 90° with the accuracy of ±0.1°.

The misalignment of M3 and M4 deteriorates the image quality but can be systematically estimated by investigating the shape of the Point Spread Function (PSF), especially spot images of the pinhole array at the defocus position. Figure 6 shows the optical simulation of the spot images in the Mg II h & k lines under perfectly aligned the CLASP2 spectro-polarimeter. We find that the five spot images along the slit show the symmetrical shape with respect to the central pinhole image. On the other hand, the optical simulation performed under the misalignment of M3 or M4 shows that their misalignments introduce the deterioration of the image quality as shown in (Figure 7). The symmetrical pattern of the spot images is easily broken when the Y-tilt has the misalignment, while the misalignment of the X-tilt can lead to astigmatism in the image, especially at the central pinhole image. These simulation results were used for the reference to diagnose the misalignment of M3 and M4.

One of the notable points from the simulation is that the misalignment of M3 and M4 degrades the image quality almost identically. Therefore, first, we need to distinguish the effects of the misalignment of M3 and M4, respectively. To clear this issue, we used two different camera brackets during the alignment of the CLASP2 spectro-polarimeter: one is a CLASP1 camera bracket (upper panel in Figure 5), the other is a new camera bracket (bottom panel in Figure 5) for CLASP2. The CLASP1 camera bracket only includes a reflective polarization analyzer whose surface is plane. Therefore, the image quality in this experiment configuration is only determined by the X- and Y-tilts of M3. First, we obtained the spot images at the defocus position by illuminating the He-Ne laser (632.8 nm) to the pinhole array installed at the slit position. Figure 8 shows one of the samples of

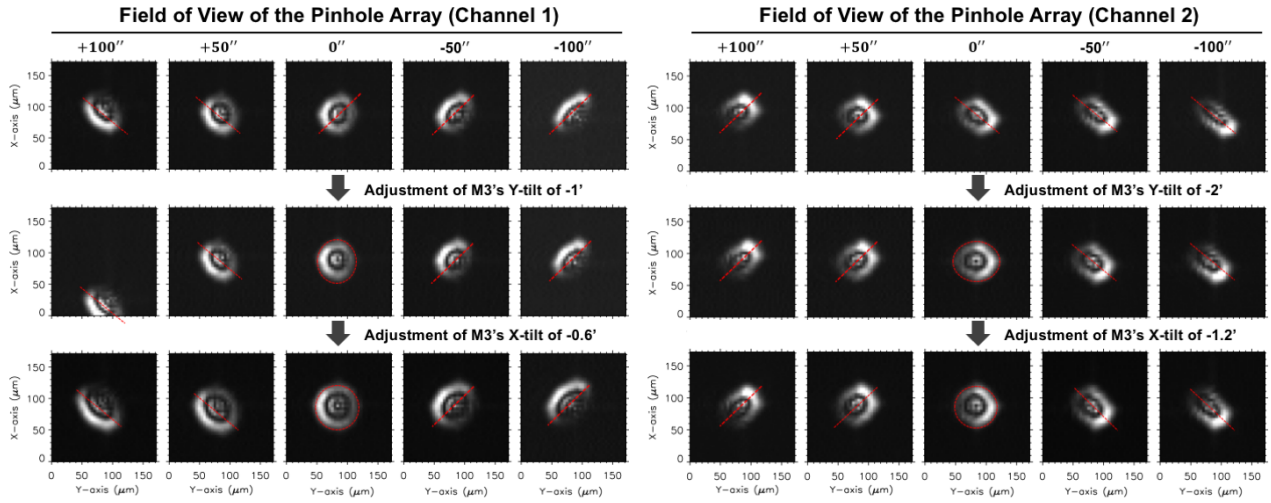

Figure 8. One sample of the adjustment of the M3's X- and Y-tilts for the channel 1 (left) and the channel 2 (right) by using the He-Ne laser (632.8 nm). The five pinhole images ($\pm 100''$, $\pm 50''$, $\pm 0''$ along the slit direction) were taken at the defocus position of -700 μm from the best focus position of the CCD cameras. The adjustment of M4's X- and Y-tilts also show the same behaviours.

the adjustment of M3's X- and Y-tilts for both the channels. We adjusted the M3's tilts by shimming under the mirror holder based on the simulation results and trial and error. The final values used to adjust the X- and Y-tilts of M3 are respectively -0.6′ (-1.2′) and -1.2′ (-2.0′) at the channel 1 (channel 2) of the spectro-polarimeter. After adjusting M3, we replaced the CLASP1 camera bracket with the CLASP2 camera bracket that M4 and M5 were installed. In this experiment configuration, the image quality is only affected by the X- and Y-tilts of M4. The variations in the shape of spot images due to the misalignment of M4's X- and Y-tilts appear the same behaviors as the variations seen in M3. During the M4'salignment, we found that M4 was largely tilted in the X- and Y-directions, which values are +120′ (+100′) and +46′ (-20′) for the channel 1 (channel 2). We adjusted M4 by shimming with reference to the optical simulation results and trial and error.

We adjusted the M5's X- and Y-tilts to shift the image position to the center of the field-of-view (FOV) of the cameras: the M5's X tilt leads to the image shift along the Y-direction (X Image shift (μm) = M5's Y tilt (′) / 0.014), and the M5's Y-tilt indrodues the image shift along the X-direction (Y Image shift (μm) = −M5's X tilt (′) / 0.013). We also use the Z-shift of M5 to adjust the focus position to the center of the focusing range of the camera. The focus position moves to twice of the M5's Z-shift distance. We moved the pinhole image to near the center of the GSE camera's FOV and focusing range by adjusting the M5's tilts and Z-shift. Finally, we adjusted a focus position of the GSE camera along the Z-axis.

3.3 Alignment with the Flight Grating

After the SP alignment using the VL grating, we replaced the VL grating with the flight grating. The X- and Y-tilts of the flight grating were adjusted with respect to the SP mechanical axis by using the theodolite and the mirror-target as like the VL grating case. The difference of X- and Y-tilts between the SP mechanical axis and the flight grating after the alignment is 0.18′ and 0.21′, respectively. These values are smaller than our tolerance ranging of 0.3′. After then, we changed the experiment configuration from the SP dolly (upper panel in Figure 4) to another dolly ("CLASP dolly" in bottom panel in Figure 4) and installed the Mg hollow cathode lamp and the UV LED lamp. By using these two lamps, we obtained the pinhole array image indicating the slit direction and the dispersion image for the alignment of the grating's Z-tilt (Figure 9). We adjusted the Z-tilt of the grating so that the angle between slit direction and the dispersion direction became about 90° with the accuracy of ±0.1°.

After the alignment of the flight grating, we obtained pinhole images at the defocus positions of the GSE camera by using the Mg hollow cathode lamp to diagnose the misalignment of the mirrors of M4 and M5. The

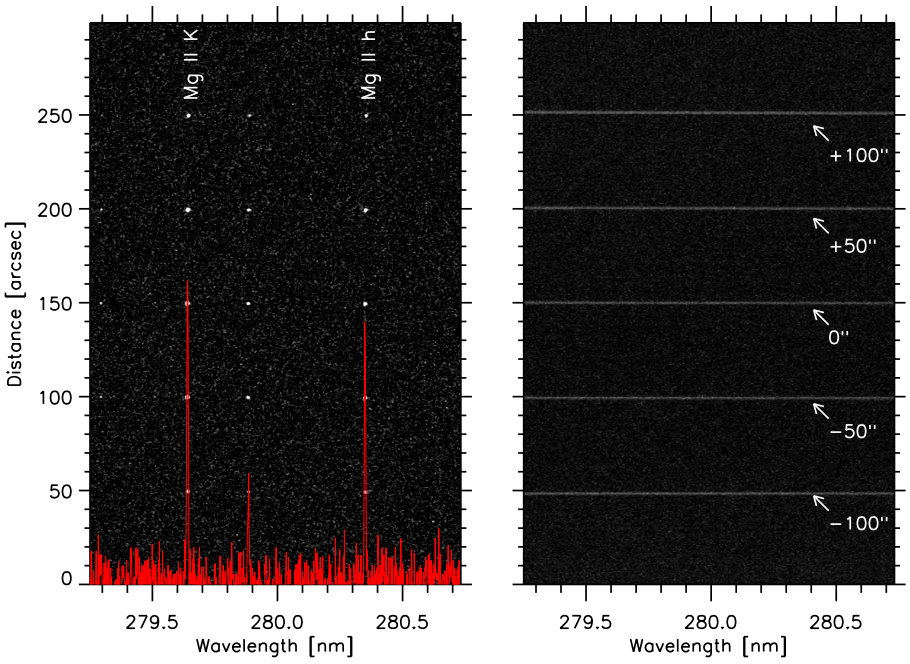

Figure 9. A pinhole array image (left) and a dispersion image (right) taken by the Mg hollow cathode lamp and the UV LED lamp.

Mg hollow cathode lamp has several emission lines near the 280 nm wavelength (Figure 9), but it is so faint that we set a long exposure time of 10 minutes to get the data by using the GSE cameras and combined ten images to increase the signal to noise. Even though our alignment by using the VL grating had been successfully conducted, we found that a slight deterioration of the image quality remains in the Mg II k line (279.64 nm). The RMS spot images we obtained have astigmatism and the asymmetry with respect to the center of the pinhole array. To remove such misalignment, we performed further fine adjustment of the X- and Y-tilts of M4 referring the optical simulation results. The final re-adjusted values of the M4's tilts in the X- and Y-directions are $+80'$ ($+60'$) and $+32'$ ($+20'$) for each channel. Meanwhile, the X- and Y-shifts of the pinhole image occurred in the FOV of the GSE camera due to the additional adjustment of the Y- and X-tilts of M4. We alsor re-adjusted the X- and Y-tilts and Z-shift of M5 in the same way as described in Section 3.2 in order to place the center of Mg II h & k spectral lines near the FOV center of the GSE camera. The final position of the Mg II h & k spectral lines is located less than 0.6 mm in the X and Y directions from the FOV center of the GSE camera. These values are less than 2.0 mm that is the adjustable range in the X and Y directions by using the flight CCD (13 μm pixel).

Figure 10 shows the final RMS spot images at the Mg II k line (279.64 nm) in both the channels. The spot size was computed by the 2D Gaussian function. The RMS spot radius at all of FOV of the slit is less than 13 μm. This satisfies our requirement of less than 13 μm at both the edges of the slit. Based on this finding, it can be seen that our alignment procedure was successfully conducted.

4. SUMMARY AND DISCUSSION

We have established and performed an efficient optical alignment procedure of the CLASP2 spectro-polarimeter. The CLASP2 spectro-polarimeter was refurbished with minimal modification from the CLASP1 instrument in order to measure the four Stokes parameters by using the Mg II h & k lines near the 280 nm. For this, we newly fabricated the SP flight mirrors and grating and performed the coating in order to increase the reflectivity at the Mg II lines. Based on our SP alignment flow shown in Figure 3, we adjusted eleven degrees of freedom in the spectro-polarimeter for each channel. During the experiment, we used defocused images to diagnose the misalignment of the spectro-polarimeter. It gave us useful information about the image quality. The alignment

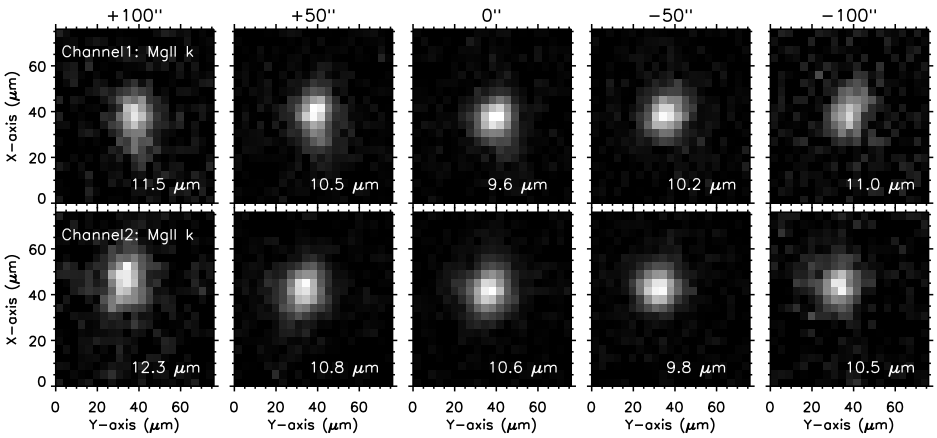

Figure 10. Final spot images in the Mg II k line of the channel1 (top) and the channel2 (bottom) obtained after the SP alignment.

of CLASP2 spectro-polarimeter raised technical difficulties, as the degrees of freedom for the optics increased compared to CLASP1 due to the addition of the new magnifier optical system. In addition, because of the low intensity of the Mg hollow cathode lamp, we first performed the alignment as much as possible with the VL grating and two kinds of camera brackets of CLASP1 and CLASP2 for the alignment of M3 and M4. After the VL alignment, the VL grating was replaced by the flight grating, and the SP alignment was performed in detail by using the Mg hollow cathode lamp. The final spot images of the CLASP2 spectro-polarimeter are seen in Figure 10. The maximum RMS spot radius at the edge of the pinhole array ($\pm 100''$) is about 12.3 μm. These measured values of the RMS spot radius are slightly overestimated compared to the real RMS spot radius because of the influence of pinhole array. It suggested that our final configuration of the spectro-polarimeter well-satisfy our requirement of the RMS spot radius of less than 13 μm at the edges ($\pm 100''$) of the slit in both channels.

Even though we achieved a satisfactory RMS spot radius for the requirement of the CLASP2 through our alignment procedure, one may wonder (1) why M4 has a larger tilt values as a reference of the X- and Y-axes and (2) why the Mg II image quality deteriorates after VL alignment. A possible explanation for the issue in (1) is that the image shift occurred in the X- and Y-directions respect to the center position of the GSE camera. After M3's alignment, we found that there was an image shift of 1.3 mm (0 mm) and 3.2 mm (1.7 mm) in the X- and Y-direction of the channel 1 (channel 2). Such an image shift suggests that the beam incident on M4 can be shifted with respect to the M4 center. It is conceivable that large M4 tilt was required to compensate the shift. We found from the optical simulation results that the M4's X-tilt of -100′ can compensate the beam shift to 2.9 mm in the Y-direction. Regarding the issue of (2), we investigated the Point Spread Function (PSF) constructed by the optical simulations with the VL grating and the flight grating. From the simulation results, we found that the Airy disk size of the He-Ne line (632.8 nm) is twice larger than that of Mg II line (280 nm). One possible explanation is that this makes it difficult for us to diagnose the shape of the defocus images taken with the He-Ne line. Figure 11 shows the PSF at the defocus images in the He-Ne line and the Mg II k line, when M4 has the tilt of -40′ as a reference of X- and Y-axes. Although we artificially gave a tilt value of -40′ to M4, the spot shape of the defocus image in the He-Ne line appears a circular-like shape different from the spot shape in the Mg II k line. It seems that the alignment of M4 using the defocus image shape in the Mg k line is more efficient than the alignment of M4 using the defocus image shape in the He-Ne line.

In conclusion, we reported on the methods and results performed the efficient alignment for the CLASP2 spectro-polarimeter. Our results show that the SP performance satisfies our requirements, i.e., the RMS spot radius at both the edges of the slit of less than 13 μm. We think that The SP alignent was successfully carried out based on our SP alignment procedure. In addition, we expect our experience of the CLASP2 SP alignment to be useful for the development of future advanced instruments using the UV wavelengths.

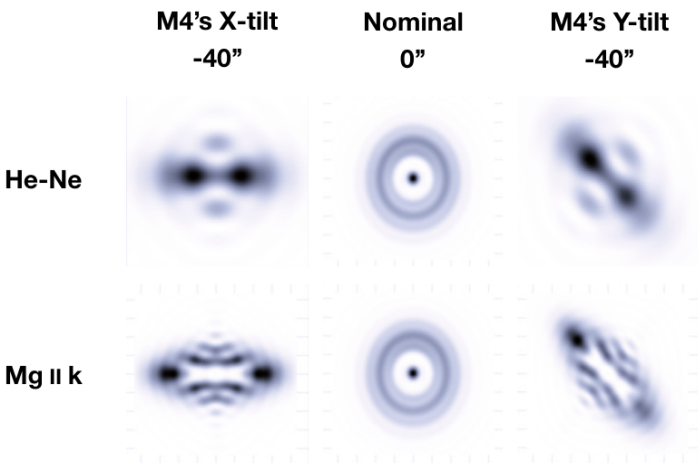

Figure 11. Point Spread Fuction of the He-Ne line (top) and the Mg II k line (bottom) at the defocus position of the CCD (focus position: -1000μm) when M4 has a misalignment of the X- and Y-titls. This was constructed by the optical simulation.

ACKNOWLEDGMENTS

We greatly appreciate the Chromospheric Lyman-Alpha Spectro-polarimeter (CLASP1) team and the the Chromospheric LAyer Spectro-Polarimeter (CLASP2) team. The CLASP1/CLASP2 teams are an international partnership between NASA Marshall Space Flight Center (MSFC) in USA, National Astronomical Observatory of Japan (NAOJ) in Japan, Japan Aerospace Exploration Agency (JAXA) in Japan, Institut d'Astrophysique Spatiale (IAS) in France, and Instituto de Astrofísica de Canarias (IAC) in Spain; additional partners are the Astronomical Institute ASCR, Istituto Ricerche Solari Locarno (IRSOL), Lockheed Martin and University of Oslo. The Japanese participation is funded by the basic research program of ISAS/JAXA, JAXA small size project program, internal research funding of NAOJ, and JSPS KAKENHI (Grant Numbers 23340052, 24740134, 24340040, 25220703, and 16H03963). The US participation is supported by the National Aeronautics and Space Administration under the CLASP2 grant issued through the Heliophysics Technology and Instrument Development for Science program. The French participation is funded by Centre National d'Etudes Spatiales (CNES). The Spanish participation is funded by the European Research Council (ERC) under the European Union's Horizon 2020 research and innovation programme (ERC Advanced Grant agreement No 742265).

REFERENCES

[1] Kano, R., Bando, T., Narukage, N., et al., "Chromospheric Lyman-Alpha Spectro-Polarimeter (CLASP)," in [*Space Telescopes and Instrumentation 2012: Ultraviolet to Gamma Ray*], *Proc. SPIE* **8443**, 84434F (Sept. 2012).

[2] Kano, R., Trujillo Bueno, J., Winebarger, A., et al., "Discovery of Scattering Polarization in the Hydrogen Lyα Line of the Solar Disk Radiation," *ApJL* **839**, L10 (2017).

[3] Ishikawa, R., Trujillo Bueno, J., Uitenbroek, H., et al., "Indication of the Hanle Effect by Comparing the Scattering Polarization Observed by CLASP in the Lyα and Si III 120.65 nm Lines," *ApJ* **841**, 31 (2017).

[4] Narukage, N., McKenzie, D., Ishikawa, R., et al., "Chromospheric LAyer Spectro-Polarimeter (CLASP2)," in [*Space Telescopes and Instrumentation 2016: Ultraviolet to Gamma Ray*], *Proc. SPIE* **9905**, 99052U (July 2016).

[5] De Pontieu, B., Title, A., Lemen, J., et al., "The Interface Region Imaging Spectrograph (IRIS)," *SoPh* **289**, 2733 (2014).

[6] Belluzzi, L. and Trujillo Bueno, J., "The Polarization of the Solar Mg II h and k Lines," *ApJ* **750**, L11 (2012).

[7] Alsina Ballester, E., Belluzzi, L., and Trujillo Bueno, J., "The Magnetic Sensitivity of the Mg II k Line to the Joint Action of Hanle, Zeeman, and Magneto-optical Effects," *ApJL* **831**, L15 (2016).

[8] del Pino Alemán, T., Casini, R., and Manso Sainz, R., "Magnetic Diagnostics of the Solar Chromosphere with the Mg II h-k Lines," *ApJL* **830**, L24 (2016).

[9] Berger, T., Mudge, J., Holmes, B., et al., "Design and fabrication of the near- ultraviolet birefringent Solc filter for the NASA IRIS solar physics mission," in [*In Current Developments in Lens Design and Optical Engineering XIII*], *Proc. SPIE* **8486**, 84860 (2012).

[10] Kubo, M., Katsukawa, Y., Suematsu, Y., et al., "Discovery of Ubiquitous Fast-Propagating Intensity Disturbances by the Chromospheric Lyman Alpha Spectro-Polarimeter (CLASP)," *ApJ* **832**, 141 (2016).

[11] Ishikawa, S., Kubo, M., Katsukawa, Y., et al., "CLASP/SJ Observations of Rapid Time Variations in the Lyα Emission in a Solar Active Region," *ApJ* **846**, 127 (2017).

[12] Giono, G., Katsukawa, Y., Ishikawa, R., et al., "Optical alignment of the Chromospheric Lyman-Alpha Spectro-Polarimeter using Sophisticated Methods to Minimize Activities under Vacuum," in [*Space Telescopes and Instrumentation 2016: Ultraviolet to Gamma Ray*], *Proc. SPIE* **9905**, 99053D (July 2016).